

Supporting Information

Article title: Modeling the mechanisms of coastal vegetation dynamics and ecosystem responses to changing water levels

Junyan Ding,¹ Nate McDowell^{2,3}, Vanessa Bailey², Nate Conroy,⁴ Donnie J. Day,⁵ Yilin Fang,⁶ Kenneth M. Kemner,⁷ Matthew L. Kirwan,⁸ Charlie D. Koven,⁹ Matthew Kovach,⁵ Patrick Megonigal,¹⁰ Kendalynn A. Morris,¹¹ Teri O'Meara,¹² Stephanie C. Pennington,¹¹ Roberta B. Peixoto,⁵ Peter Thornton,¹² Mike Weintraub,⁵ Peter Regier,¹³ Leticia Sandoval,⁵ Fausto Machado-Silva,⁵ Alice Stearns,¹⁰ Nick Ward,¹³ Stephanie J. Wilson¹⁰

Article acceptance date: [Click here to enter a date.](#)

The following Supporting Information is available for this article:

Tables:

Table S1 List of major parameters of FATES-Hydro

Table S2 Marsh plant (grass) parameters

Table S3 measured %NSC in 2022 at Lake Erie site

Figures:

Fig S1. Google Earth photos of the upland broadleaf forest at Lake Erie site (a) and conifer forest at Chesapeake Bay site (b).

Fig. S2 Saturation-induced root loss function, showing different root loss rates for plants not adapted to water-logging environments (solid blue line) and plants more adapted to water-logging environments (dashed red line). The solid blue line represents the root loss rate used in this study, controlled by specific parameters.

Fig S3. Observed and simulated hourly leaf net carbon assimilation rate (Anet) and leaf water potential (LWP) at upland and shoreline locations at Lake Erie site on July 15th. 2022

Fig S4. Measured and simulated hourly sap flow of upland (top) and shoreline (bottom) broadleaf trees during 2022 growing season at Lake Erie

Fig S5. Comparison of simulated growth rate and measured growth rate from tree cores at shoreline location (top) and upland location (bottom)

Table S1 List of major tree parameters of FATES-Hydro

Symbol	Source code name	Value			Description	Source
		Conifer tree	Broad leaf tree	Units		
P50gs	fates_hydr_p50_gs	-2.0	-1.6	MPa	Leaf xylem water potential at half stomatal closure	Wang et al., 2021, this study
a _{gs}	fates_hydr_avuln_gs	5	3.5	unitless	shape parameter for stomatal closure	Wang et al., 2021, this study
K _{max}	fates_hydr_kmax_node	0.7	1.0	kg/MPa/m/s	Maximum xylem conductivity per unit sap area	Ding et al. 2023b, this study
A	fates_hydr_vg_alpha_node	0.198392	0.07113	Mpa ⁻¹	Shape parameter of van Genuchten plant hydraulic model when soil PSU=0	Ding et al. 2023b, this study
m, n	fates_hydr_vg_m_node fates_hydr_vg_n_node	0.866, 2.765	0.8, 1.25	unitless	Shape parameter of van Genuchten plant hydraulic model when soil PSU=0	Ding et al. 2023b, this study
dA, dn	fates_hydr_vg_da_sal fates_hydr_vg_dn_sal	-0.00651 -0.122193	-0.0065 -0.1222	unitless	change of A and n of plant hydraulic model per unit PSU	Ding et al. 2023b
χ	fates_hydr_p_taper	0.333	0.333	unitless	xylem taper exponent	Christoffersen et al., 2016
RWC _{res,l} , RWC _{res,s} , RWC _{res,r}	fates_hydr_resid_node	0.25, 0.325, 0.15	0.16,0.21, 0.21	proportion	residual fraction of leaf, stem, root	Christoffersen et al., 2016
Θ _{sat,x}	fates_hydr_thetas_node	0.65	0.72	cm ³ /cm ³	saturated water content of xylem	Christoffersen et al., 2016

SLA_{max}	fates_leaf_slamax	0.014	0.0185	m^2/gC	Maximum Specific Leaf Area (SLA)	This study
SLA_{top}	fates_leaf_slatop	0.014	0.0185	m^2/gC	Specific Leaf Area (SLA) at top of canopy, projected area basis	This study
$V_{cmax,25,top}$ (PSU=0)	fates_leaf_vcmax25top	50	47	$\mu mol CO_2/m^2/s$	maximum carboxylation rate of Rub. at 25C, canopy top	This study
g_0	fates_leaf_stomatal_intercept	10000	10000	$\mu mol H_2O/m^2/s$	Minimum leaf stomatal conductance	calibrated
ra, rb	fates_fnrt_prof_a fates_fnrt_prof_b	0.6, 1	0.6, 1	unitless	Root distribution parameters	Ding et al. 2023b
b	fates_hydr_frt_loss_coe	1	1	unitless	Saturation root loss par.	calibrated
k_s	fates_hydr_frt_loss_exp	0.02	0.02	unitless	Saturation root loss par.	calibrated
k_{ex}	fates_hydr_k_salex	0.80	0.80	ratio	root salt exclusion ratio	Ding et al. 2023b
kr_{sal}	fates_hydr_frt_loss_salk	0.0000075	0.0000075	unitless	salinity root loss rate par.	Ding et al. 2023b
cr_{sal}	fates_hydr_frt_loss_salkr	3.5	3.5	PSU	salinity root loss threshold	Ding et al. 2023b
m_{cs}	fates_mort_scalar_starvation	1.2	1.2	N/N/Year	maximum carbon starvation mortality rate	Ding et al. 2023b
m_{hf}	fates_mort_scalar_hydraulic_failure	1.2	1.2	N/N/Year	maximum hydraulic failure mortality rate	Ding et al. 2023b

Table S2 Marsh plant (grass) parameters

Parameter	description	value	unit	source
w_max	maximum width	35	cm	this study
bl2w_slp	slope of leaf biomass to width power law function	0.0747	unitless	this study
bl2w_exp	exponent of leaf biomass to width power law function	2.1555	unitless	this study
h2w_slp	slope of height to width power law function	41.96	unitless	this study
h2w_exp	exponent of height to width power law function	0.5126	unitless	this study
bbslope	Ball-Berry leaf conductance slope	9	unitless	O'Meara et al., 2021
bbopt	Ball-Berry minimum leaf conductance	10000	$\mu\text{mol H}_2\text{O}/\text{m}^2/\text{s}$	O'Meara et al., 2022
Vcmax,25	maximum carboxylation rate of Rub. at 25C	55	$\text{mmol CO}_2/\text{m}^2/\text{s}$	O'Meara et al., 2023
SLA	specific leaf area	0.04	m^2/gC	O'Meara et al., 2024

Table S3 measured %NSC in 2022 at Lake Erie site

Location		Glucose	Fructose	Sucrose	Starch	Total
upland	foliage	0.159%	0.122%	3.469%	0.334%	4.084%
	wood	0.041%	0.367%	2.603%	1.426%	4.437%
shoreline	foliage	0.157%	0.155%	5.024%	0.850%	8.521%
	wood	0.031%	0.405%	3.423%	2.459%	6.319%

Fig S1. © Google Earth photos of the upland broadleaf forest at Lake Erie site (a) and conifer forest at Chesapeake Bay site (b).



Fig. S2 Saturation-induced root loss function, showing different root loss rates for plants not adapted to water-logging environments (solid blue line) and plants more adapted to water-logging environments (dashed red line). The solid blue line represents the root loss rate used in this study, controlled by specific parameters.

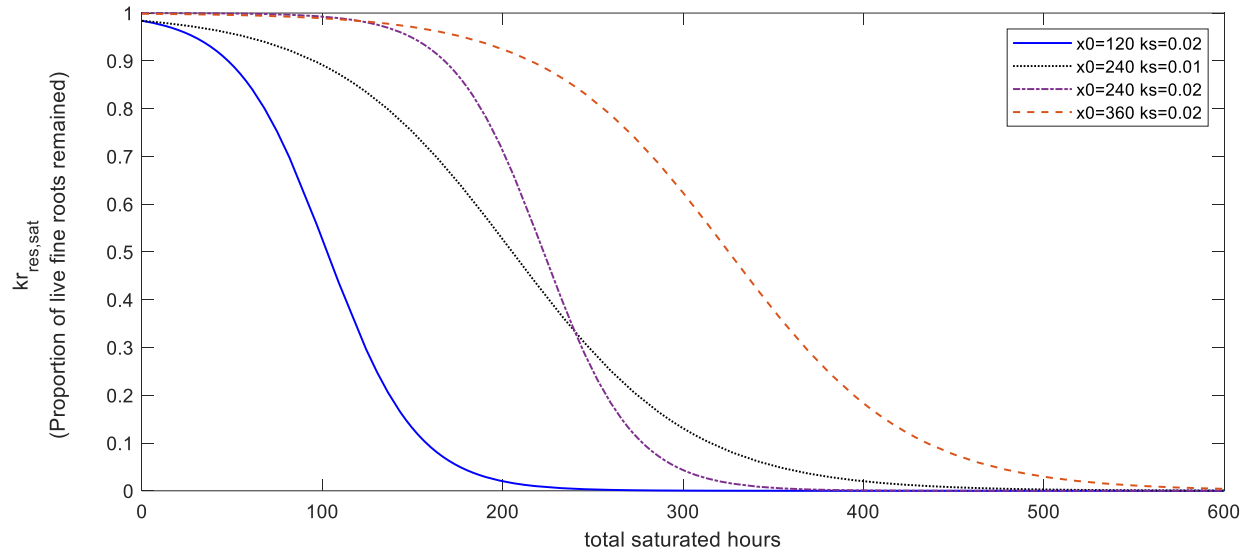


Fig S3. Observed and simulated hourly leaf net carbon assimilation rate (Anet) and leaf water potential (LWP) at upland and shoreline locations at Lake Erie site on July 15th, 2022

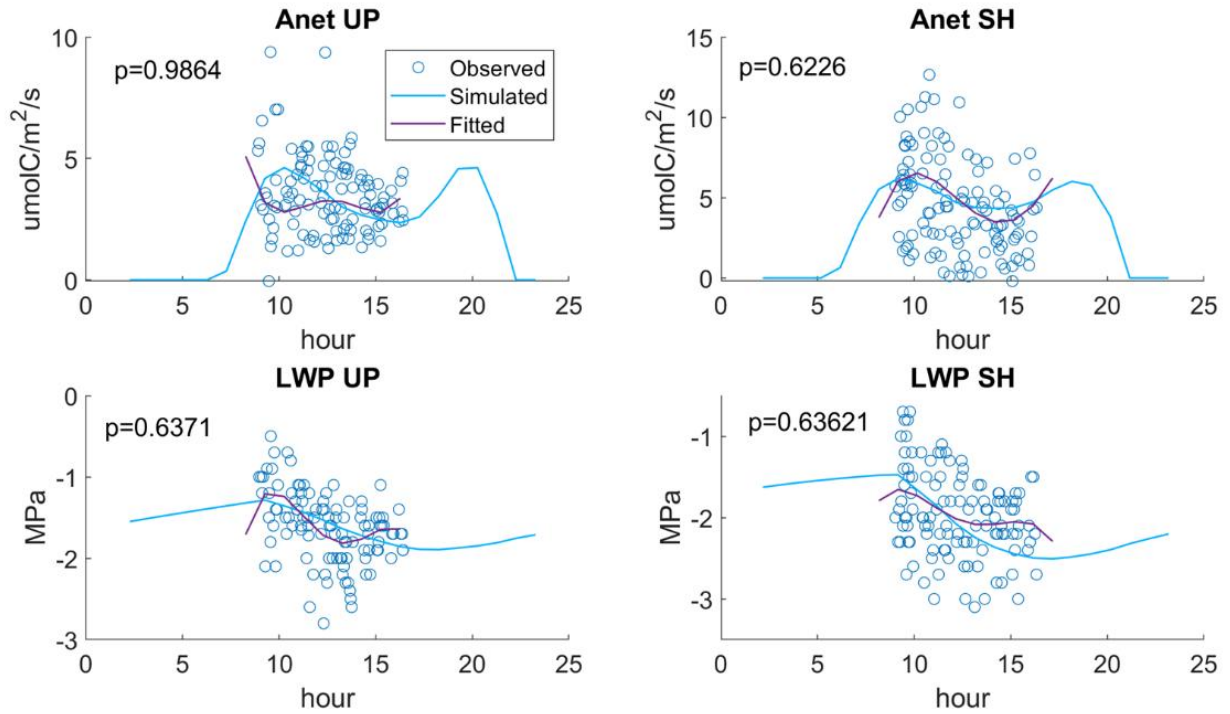


Fig S4. Measured and simulated hourly sap flow of upland (top) and shoreline (bottom) broadleaf trees during 2022 growing season at Lake Erie

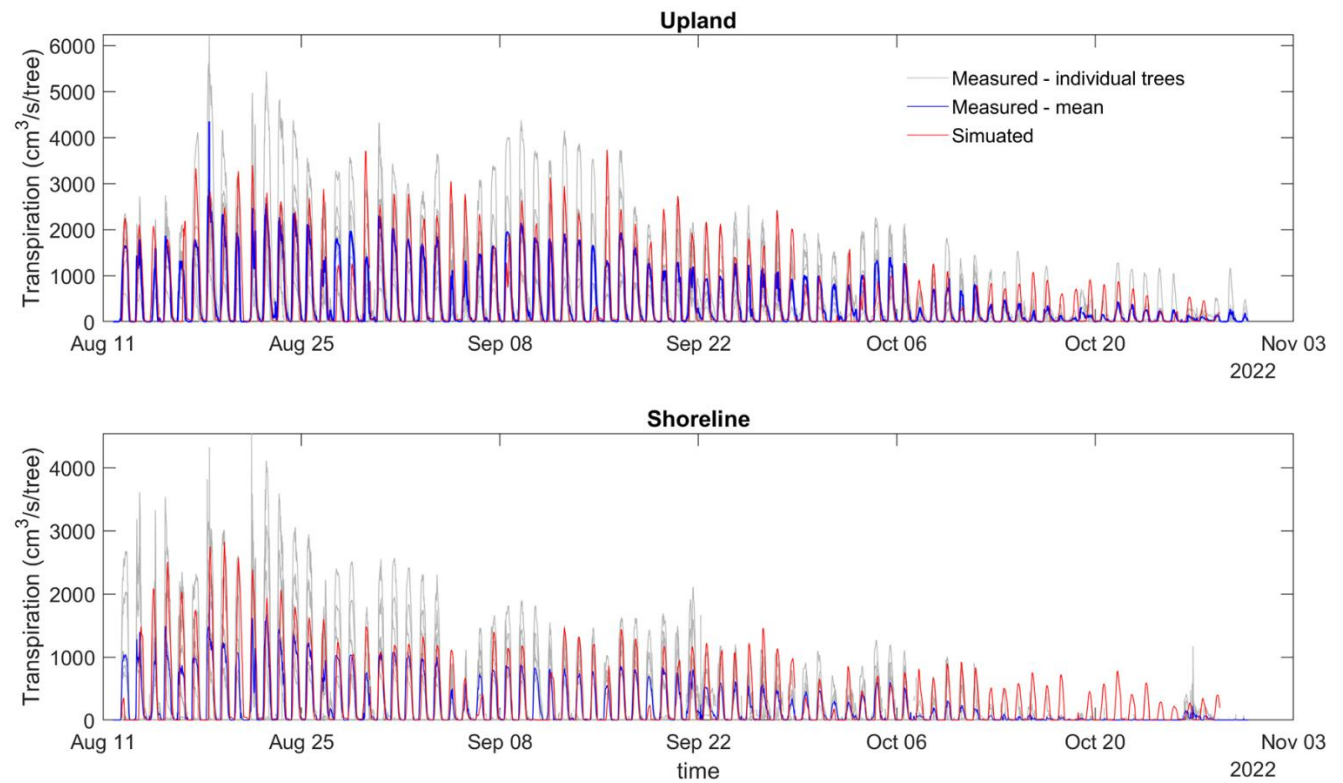


Fig S5. Comparison of simulated growth rate and measured growth rate from tree cores at shoreline location (top) and upland location (bottom)

